Pion-Nucleon Phase-Shift Analysis: 0–350 MeV*

L. DAVID ROPER AND ROBERT M. WRIGHT
Lawrence Radiation Laboratory, University of California, Livermore, California
(Received 15 January 1965)

Several sets of energy-dependent pion-nucleon phase shifts have been obtained in the 0–350-MeV energy range. These solutions differ near the end of the energy range and in the signs and magnitudes of some of the small phases. There is very little difference among these solutions in their prediction of the observables, including the spin-rotation parameters. Some very difficult experiments are suggested to distinguish among the solutions.

I. INTRODUCTION

AN extensive pion-nucleon phase-shift analysis is in progress at Livermore.[1] The analysis is an energy-dependent one supplemented by single-energy analyses. The parametrization used, the search procedure, and various stages of progress have been reported elsewhere.[1]

The first part of the program was an analysis in the 0–350-MeV energy range. This then served as a starting point for a 0–700-MeV analysis.[1] The advent of theoretical predictions of the 0–350-MeV pion-nucleon phase shifts[2,3] has led us to examine more closely the 0–350-MeV solutions. We find that precise measurements of hitherto unmeasured observables or of angular distributions and polarizations in hitherto unmeasured angular regions are necessary in order to distinguish among the solutions.

II. SOLUTIONS

There are three basic solutions which we differentiate by the starting points of the search. In all three solutions the Layson resonance form[4] was used for the P_{33} state (the notation is $l_{2T,2J}$). We used a selection of 576 data in the 0–350-MeV energy range.

(A) Solution A is started from the Hamilton and Woolcock scattering lengths[5] for the S_{11}, S_{31}, P_{11}, P_{31}, and P_{13} states with all other phases zero except the P_{33}. In Fig. 1 the starting curves are marked A and the output after the search is marked AO.

(B) Solution B is started from the DHL phases.[2] Since they do not predict S_{11}, S_{31}, and P_{11} phases, we use the AO values as input for these phases. In Fig. 1 the starting curves are marked B and the output after the search is marked $BO1$. Since the $BO1$ F-waves became

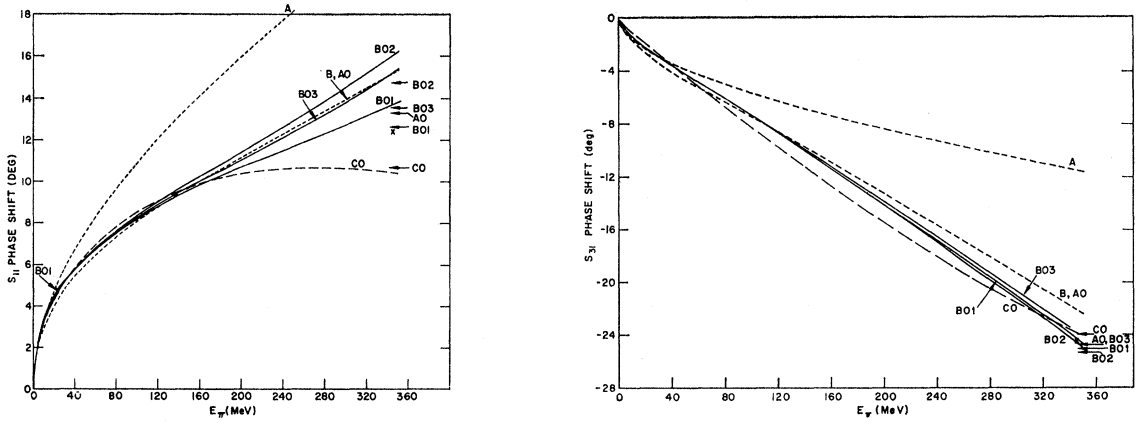

(a) (b)

FIG. 1. (a)–(n) The arrows at the right edges indicate the 345-MeV values obtained when new data were included and the real parts of the forward amplitudes were used as data. The crosses at the right-hand edges indicate the values at 345 MeV of the latest of our 300–700-MeV solutions (unpublished) (see Sec. IV). See Sec. II for explanation of the notation. FIG. 1 (*continued*)

* Work done under the auspices of the U. S. Atomic Energy Commission.

[1] L. D. Roper, R. M. Wright, and B. T. Feld, Phys. Rev. **138**, B190 (1965); B. T. Feld and L. D. Roper, in *Proceedings of the Sienna International Conference on Elementary Particles*, edited by G. Bernadini and G. P. Puppi (Italian Physical Society, Bologna, 1963), p. 400; L. D. Roper, Phys. Rev. Letters **12**, 340 (1964); L. D. Roper and R. M. Wright, Lawrence Radiation Laboratory (Livermore) UCRL-7846, 1964 (unpublished).

[2] A. Donnachie, J. Hamilton, and A. T. Lea, Phys. Rev. **135**, B515 (1964).

[3] M. Kikugawa, Progr. Theoret. Phys. (Kyoto) **31**, 656 (1964); N. Hiroshige, I. Ino, and M. Kikugawa, *ibid.* **31**, 721 (1964); H. Hiroshige and M. Kikugawa, Hiroshima University, 1964 (unpublished).

[4] W. M. Layson, Nuovo Cimento **27**, 724 (1963).

[5] J. Hamilton and W. S. Woolcock, Rev. Mod. Phys. **35**, 737 (1963).

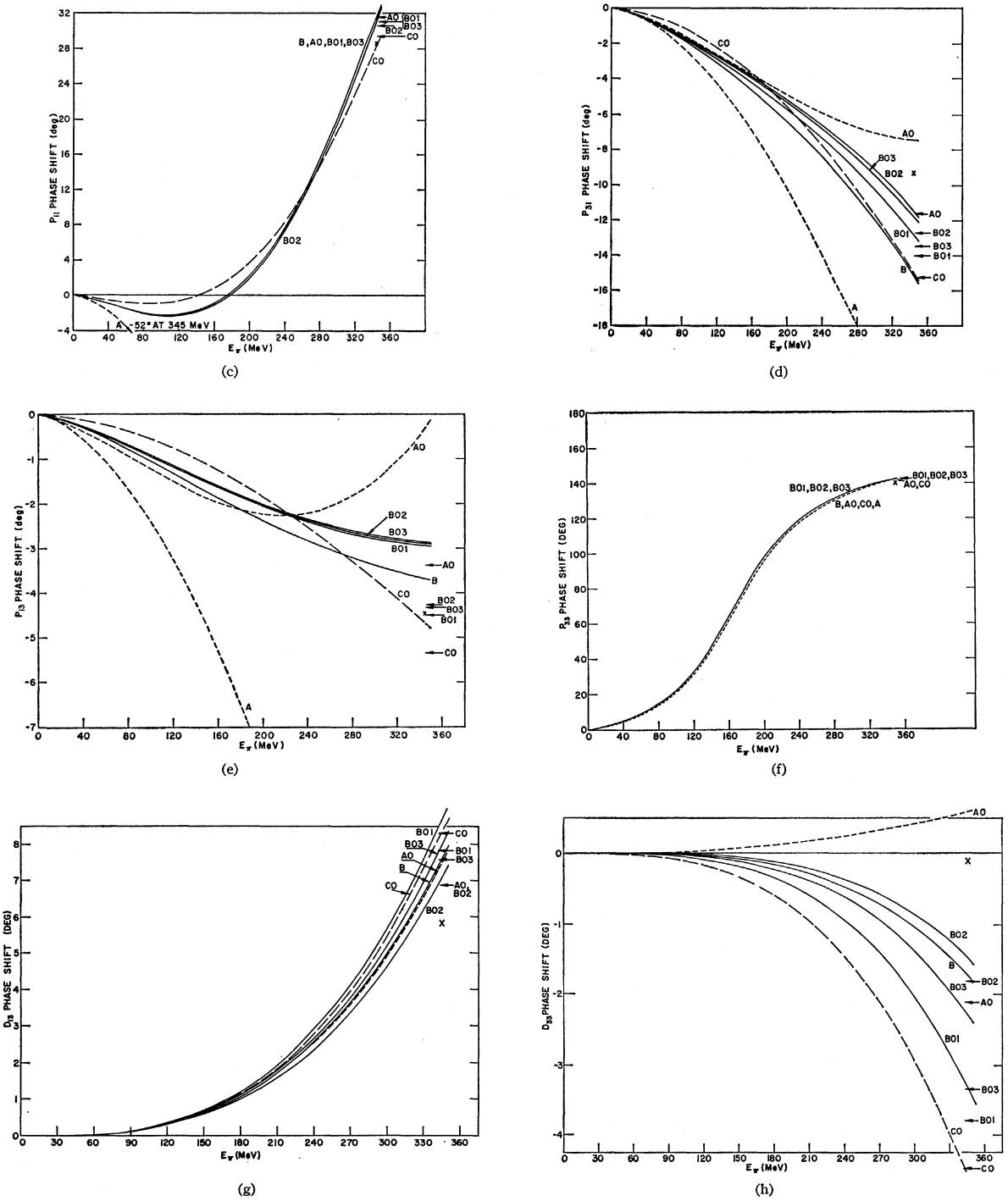

FIG. 1 (*continued*)

much larger than the B F waves, a search was made starting from B with the F waves fixed at the B values. This output is marked *BO2*. Then starting from *BO2*, the F waves were allowed to vary, which yielded *BO3*.

(C) Solution C is started with all phases zero except the P_{33} phase. The output after the search is marked *CO* in Fig. 1. The values of the phase shifts at 345 MeV for the various input and solutions given above are listed in Table I. The numerical results for solution *BO1* are given in Ref. 1.

The fact that such completely different input as described in (A), (B), and (C) above yield solutions

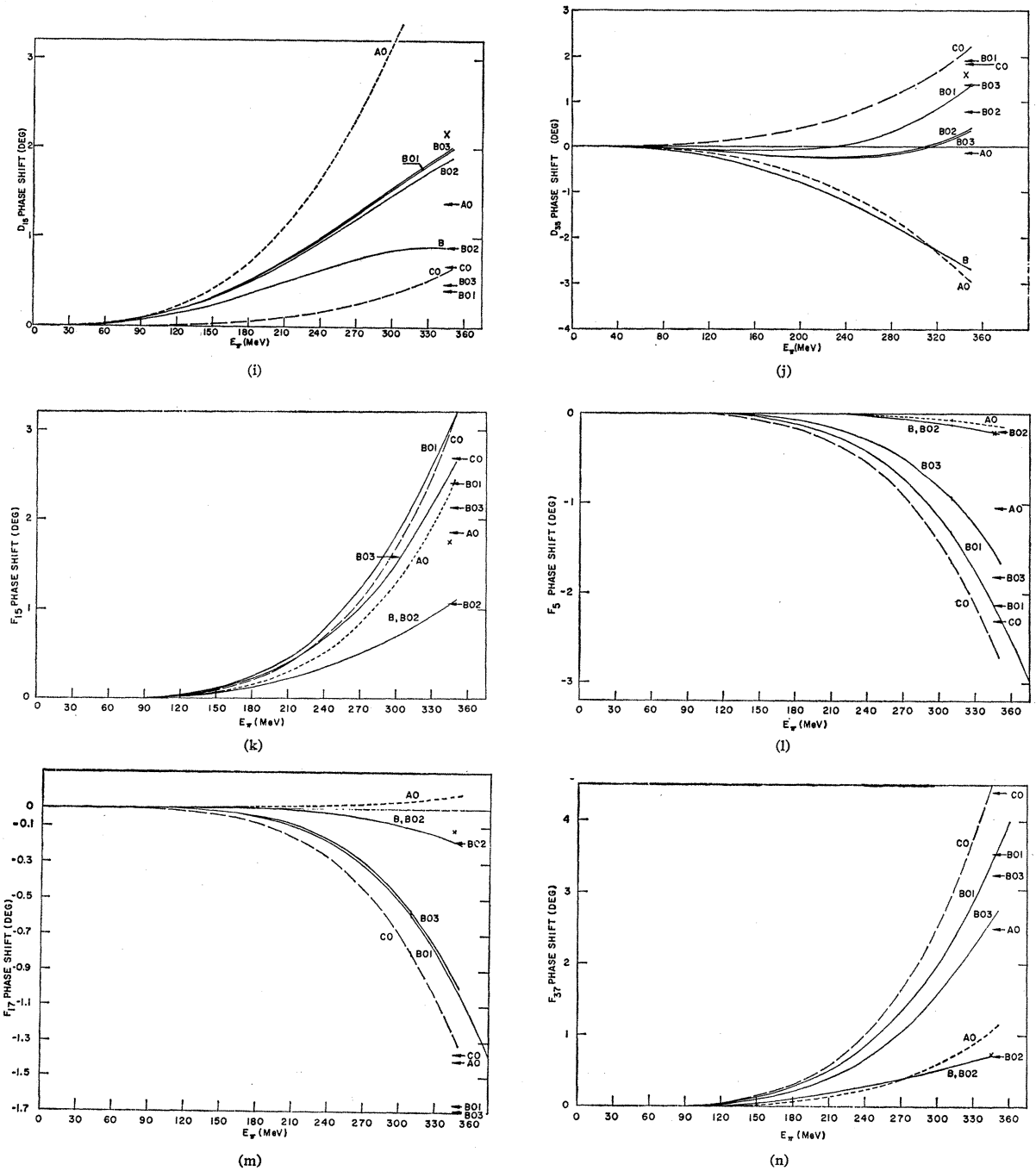

FIG. 1 (*continued*)

that are very much alike leads one to believe that the coarse features of the solutions are unique. Now the problem is reduced to selecting solutions on the basis of fine detail.

III. OBSERVABLES

We now examine the solutions to see how they differ in predicting observables that have not been measured. The complete set of angular observables are given in Figs. 2, 4, and 6 for 31, 170, and 310 MeV, respectively. Four angular observables are given for 98 MeV in Fig. 3, and two are given for 246 MeV in Fig. 5. Electromagnetic effects are included in the curves. The equations for the angular observables are:

(1) Differential cross section:

$$\sigma(\theta)=|f(\theta)|^2+|g(\theta)|^2,$$

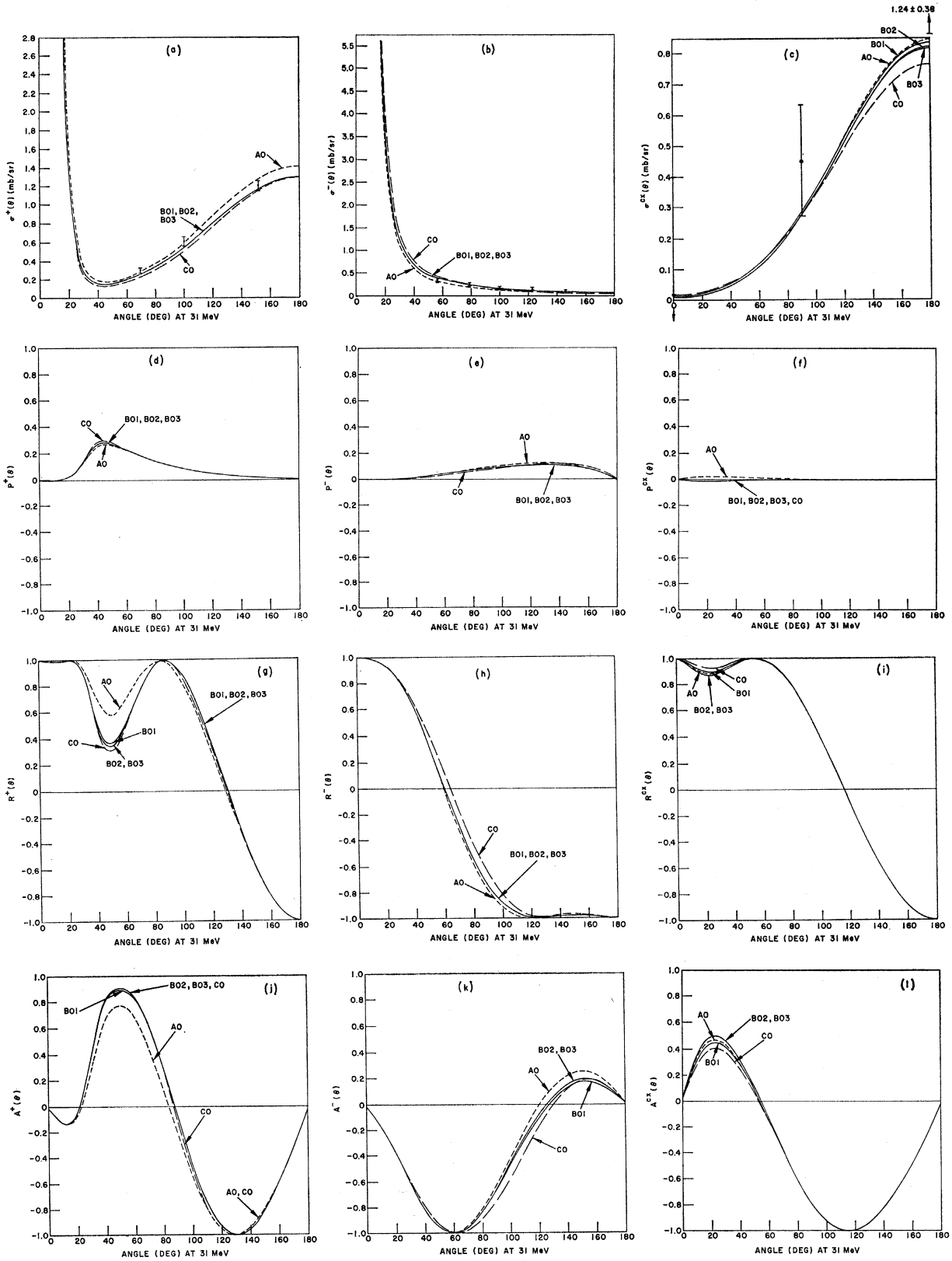

FIG. 2. The solutions' predictions for all angular observables at 31 MeV. (a) The points are 31.4-MeV data from D. E. Knapp and K. Kinsey, Phys. Rev. **131**, 1822 (1963). Renormalization of the data in the searches is not shown. (b) The points are 31.9- (at 56.4°) and 31.4-MeV data from the same source as (a). Renormalization of the data in the searches is not shown. (c) The points at 0, 90, and 180° are calculated from the 31-MeV Legendre polynomial series coefficients given by K. Miyake, K. F. Kinsey, and D. E. Knapp, Phys. Rev. **126**, 2188 (1962). Renormalization of the data in the searches is not shown.

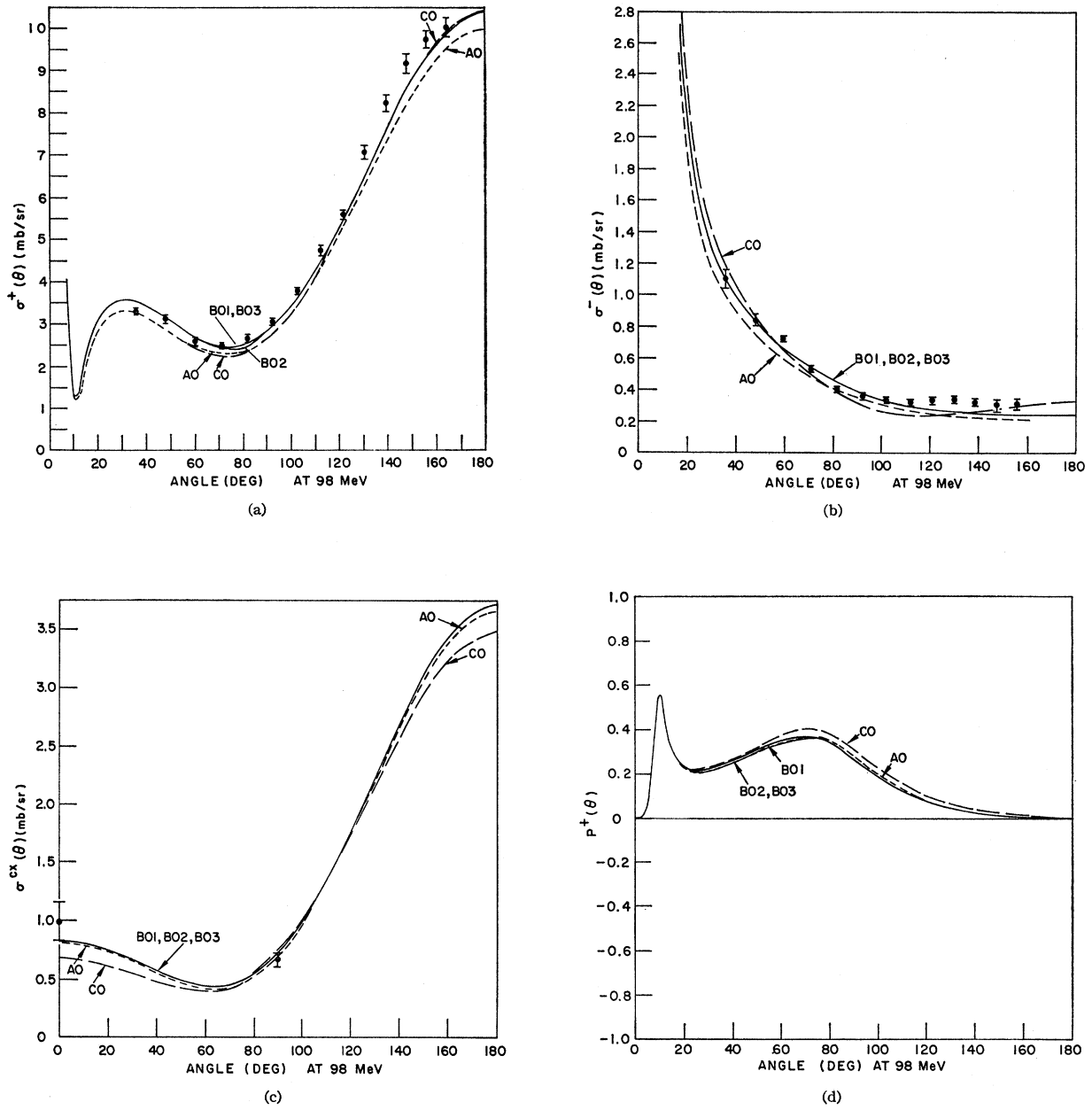

FIG. 3. The solutions' predictions for four angular observables at 98 MeV. (a) The points are 97.1-MeV data from T. Massam (Liverpool) (private communication). Note the Coulomb interference at about 11°. Renormalization of the data in the searches is not shown. (b) The points are 98-MeV data from D. N. Edwards, S. G. F. Frank, and J. R. Holt, Proc. Phys. Soc. (London) **73**, 856 (1959). Renormalization of the data in the searches is not shown. (c) The points at 0, 90, and 180° are calculated from the 96-MeV $\cos\theta$ series coefficients given by G. Myatt (Liverpool) (private communication). Renormalization of the data in the searches is not shown. (d) Note the Coulomb interference at about 11°.

where θ is the c.m. pion scattering angle.

(2) Polarization:

$$\mathcal{P}(\theta)=-2\,\mathrm{Im}[f^*(\theta)g(\theta)]\hat{n}/\sigma(\theta),$$

where $\hat{n}=(\mathbf{k}\times\mathbf{k}')/|\mathbf{k}\times\mathbf{k}'|$, $\mathbf{k}$ is the incident pion c.m. momentum, and $\mathbf{k}'$ = final pion c.m. momentum.

(3) Spin-rotation parameters[6]:

$$A(\theta)=\frac{-(|f(\theta)|^2-|g(\theta)|^2)\sin\theta-2\,\mathrm{Re}[f^*(\theta)g(\theta)]\cos\theta}{|f(\theta)|^2+|g(\theta)|^2}$$

and

$$R(\theta)=\frac{(|f(\theta)|^2-|g(\theta)|^2)\cos\theta-2\,\mathrm{Re}[f^*(\theta)g(\theta)]\sin\theta}{|f(\theta)|^2+|g(\theta)|^2},$$

[6] Y. S. Kim, Phys. Rev. **129**, 862 (1963).

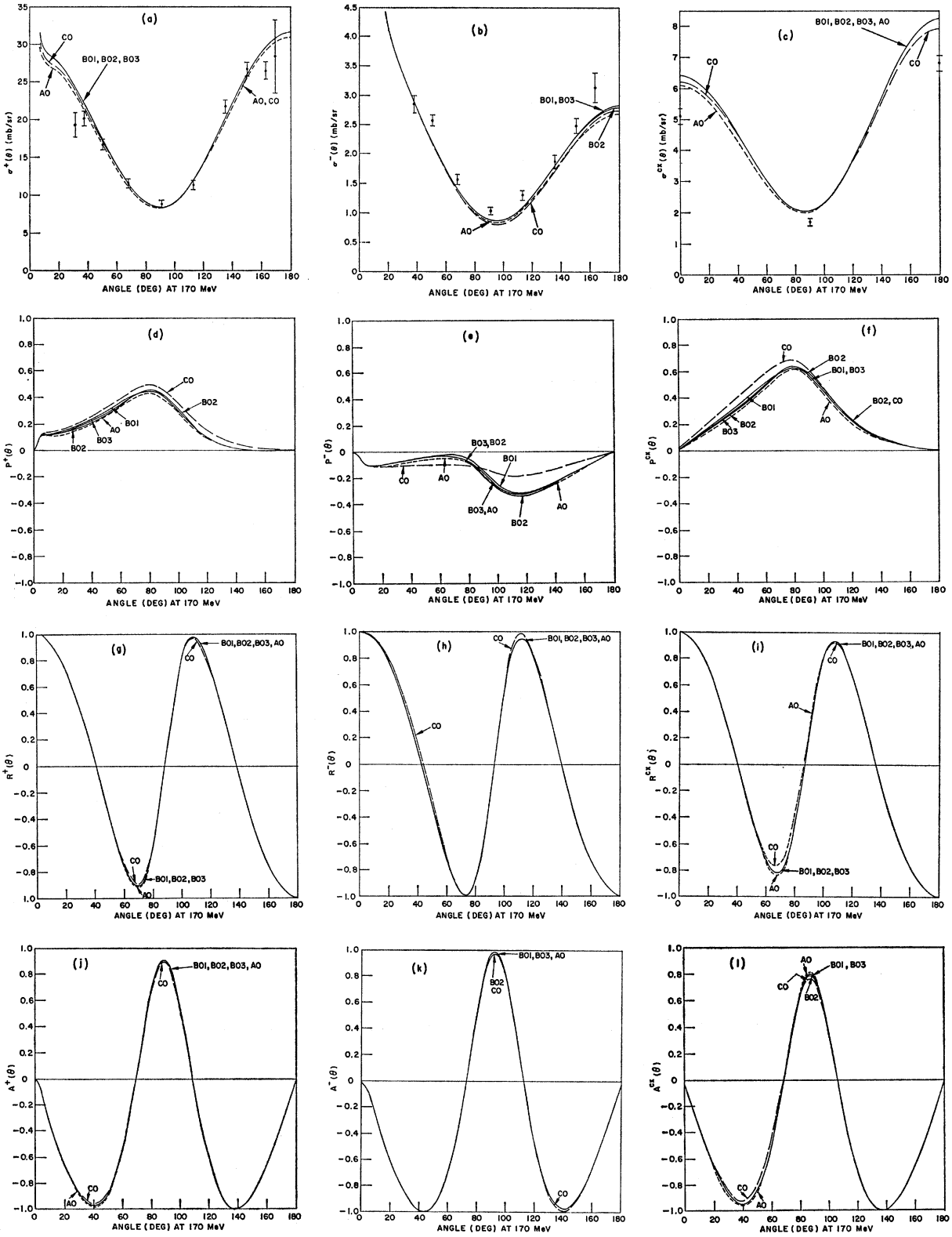

FIG. 4. The solutions' predictions for all angular observables at 170 MeV. (a) The points are 170-MeV data from J. Ashkin, J. P. Blaser, F. Feiner, and M. O. Stern, Phys. Rev. **101**, 1149 (1956). Renormalization of the data in the searches is not shown. (b) The points are 170-MeV data from the same source as (a). Renormalization of the data in the searches is not shown. (c) The points at 0, 90, and 180° are calculated from the 170-MeV $\cos\theta$ series coefficients given by the same source as (a). Renormalization of the data in the searches is not shown.

TABLE I. Values of the phase shifts at 345 MeV for the various input and solutions. The last four lines contain solution χ^2's.

Phase	A	AO	B	$BO1$	$BO2$	$BO3$	C	CO
S_{11}	21.63	15.20	15.20	13.65	16.08	15.22	0	10.44
S_{31}	−11.53	−22.13	−22.13	−24.28	−24.63	−23.84	0	−23.90
P_{11}	−51.55	31.79	31.79	31.98	31.29	31.72	0	28.47
P_{31}	−25.35	−7.46	−15.17	−12.89	−11.51	−11.82	0	−15.08
P_{13}	−19.88	−0.33	−3.69	−2.96	−2.89	−2.85	0	−4.69
P_{33}	141.17	141.17	141.17	141.63	141.62	141.62	141.17	141.21
D_{13}	0	7.49	7.60	8.73	7.09	7.94	0	8.33
D_{33}	0	0.58	−1.74	−3.32	−1.49	−2.31	0	−4.57
D_{15}	0	4.79	0.89	1.92	1.84	1.96	0	0.62
D_{35}	0	−2.85	−2.63	1.26	0.33	0.28	0	2.10
F_{15}	0	2.31	1.06	3.07	1.06	2.51	0	3.00
F_{35}	0	−0.12	−0.19	−2.14	−0.19	−1.55	0	−2.59
F_{17}	0	0.07	−0.19	−0.96	−0.19	−0.95	0	−1.26
F_{37}	0	1.06	0.72	3.41	0.72	2.62	0	4.51
χ^2	very large	1091	2050	1001	1067	1002	29 000	1043
χ^2 (expected)		548		539	547	539		543
χ^2/χ^2 (exp.)		1.99		1.86	1.95	1.86		1.92
χ^2 (renormalization)[a]		151		71	73	74		110

[a] Contribution to χ^2 due to renormalization. (See Ref. 1.)

where the non-spin-flip and spin-flip amplitudes are, respectively,

$$f(\theta)=\frac{\lambda}{k}\sum_{l=0}^{l_m}[(l+1)A_{l+}+lA_{l-}]P_l(\cos\theta)$$

and

$$g(\theta)=\frac{\lambda}{k}\sum_{l=0}^{l_m}[A_{l+}-A_{l-}]P_l^1(\cos\theta)\,,$$

and the partial-wave amplitudes are

$$A_{l\pm}=(1/2i)[\eta_{l\pm}e^{2i\delta_{l\pm}}-1]$$

in terms of the phase shifts $\delta_{l\pm}$ and the absorption parameters $\eta_{l\pm}$ for scattering in the states with $J=l\pm\frac{1}{2}$. See Ref. 1 for inclusion of electromagnetic effects. The observable amplitudes in terms of the isotopic spin amplitudes are

$$A^+=A^{(3/2)},\quad A^-=(1/3)(A^{(3/2)}+2A^{(1/2)}),$$

and

$$A=\frac{\sqrt{2}}{3}(A^{(3/2)}-A^{(1/2)})\,.$$

Figure 7 shows the charge-exchange Legendre poly-

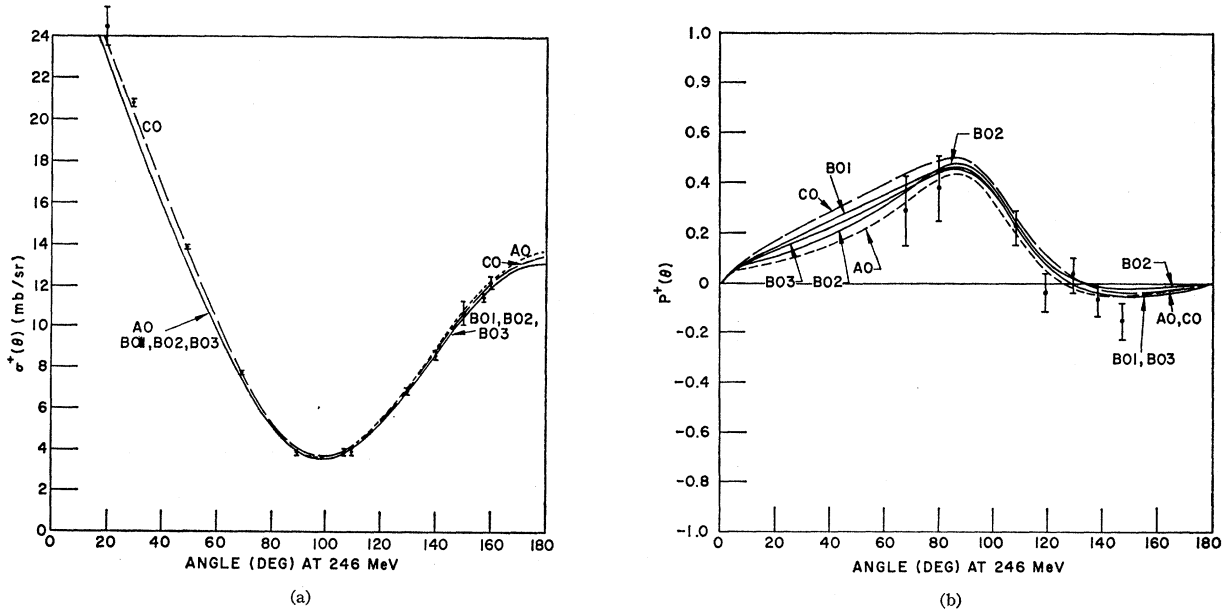

(a) (b)

FIG. 5. The solutions' predictions for two angular observables at 246 MeV. (a) The points are 247.5-MeV data from W. K. Troka, Lawrence Radiation Laboratory (Berkeley) UCRL-11537, 1964 (unpublished). These data were not used in the search. (b) The points are 246-MeV data from C. Schultz, Lawrence Radiation Laboratory (Berkeley) UCRL-11149, 1964 (unpublished).

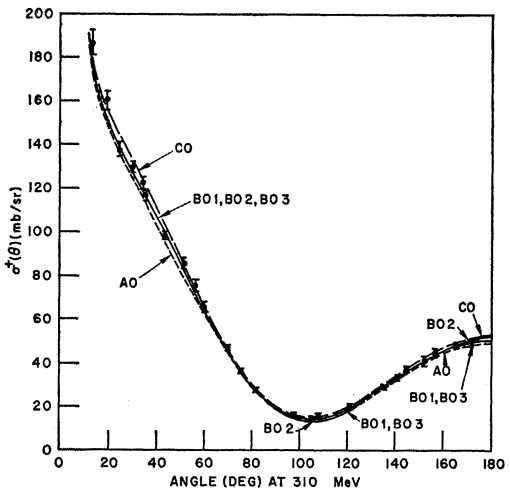

(a)

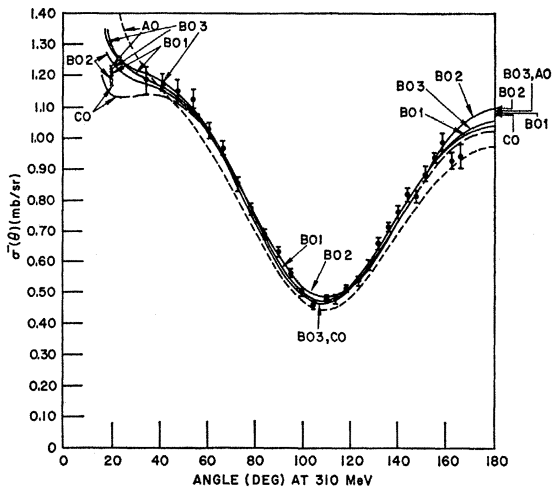

(b)

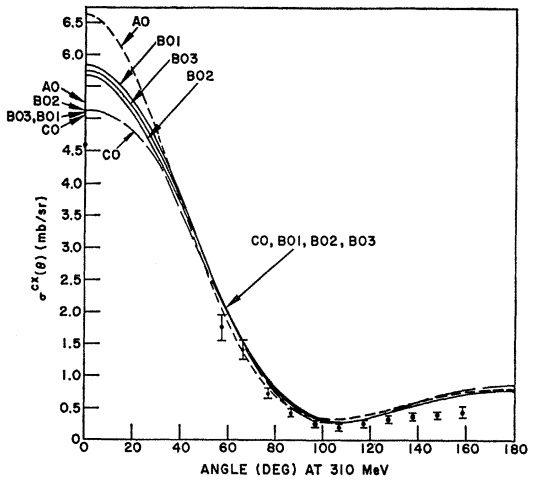

(c)

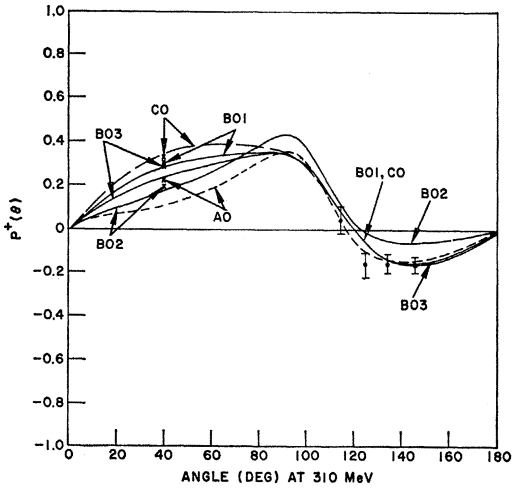

(d)

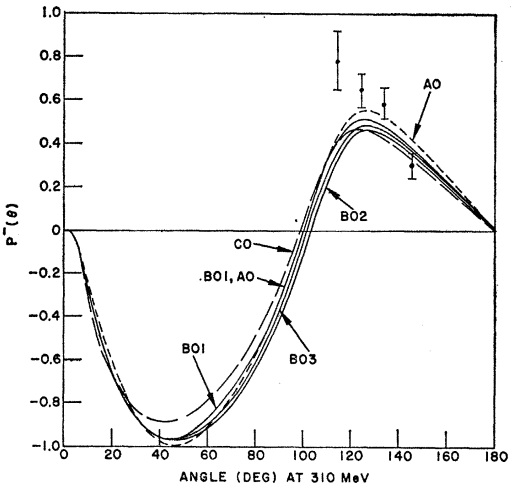

(e)

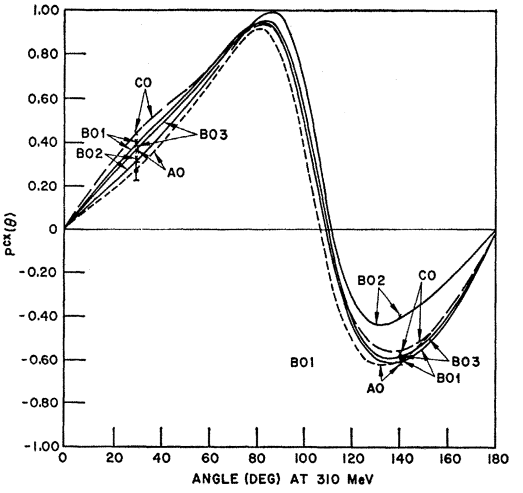

(f)

FIG. 6. The solutions' predictions for all angular observables at 310 MeV. (a) The points are 310-MeV data from J. H. Foote, O. Chamberlain, E. H. Rogers, and H. M. Steiner, Phys. Rev. **122**, 959 (1961). Renormalization of the data in the searches is not shown. (b) The points are 310-MeV data from H. R. Rugge and O. T. Vik, Phys. Rev. **126**, 2300 (1963). The arrows at the right edge and the crosses at 20° indicate how the solutions changed when new data were included and the real parts of the forward amplitudes were used as data. Renormalization of the data in the searches is not shown. (c) The points are 313-MeV data from R. J. Kurz and D. L. Lind, Lawrence Radiation Laboratory (Berkeley) UCRL-11548, 1964 (unpublished). The arrows at the left edge indicate how the solutions changed when new data were included and the real parts of the forward amplitudes were used as data. These data were not used in the

FIG. 6 (*continued*)

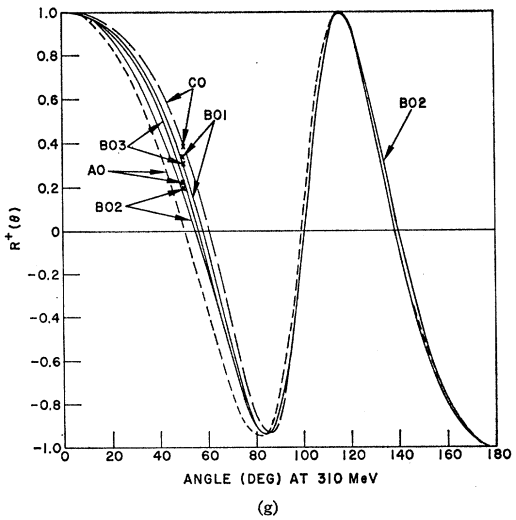

(g)

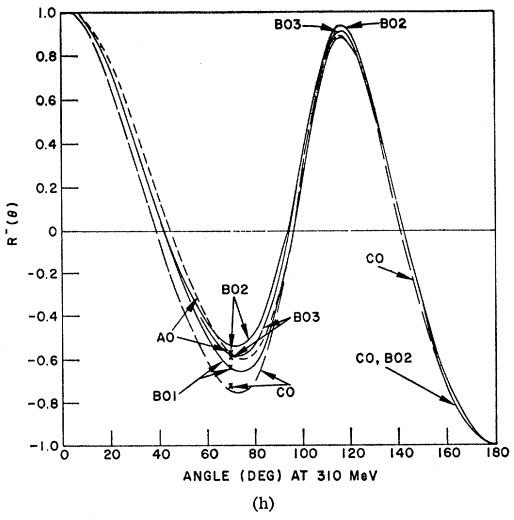

(h)

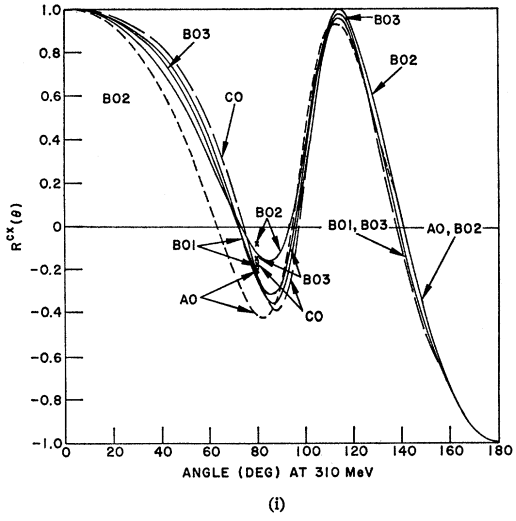

(i)

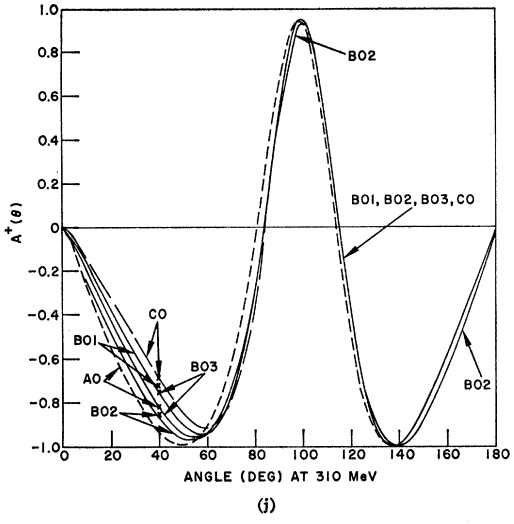

(j)

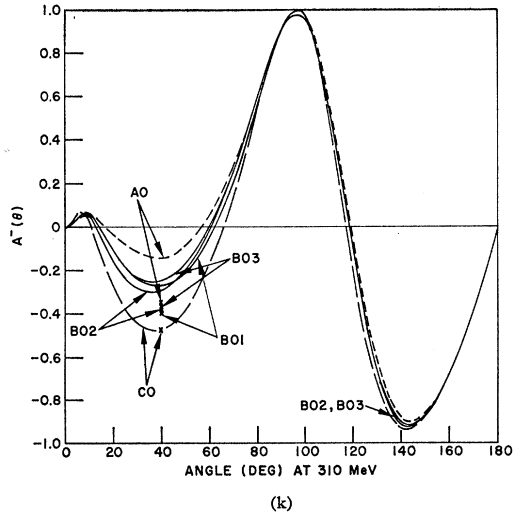

(k)

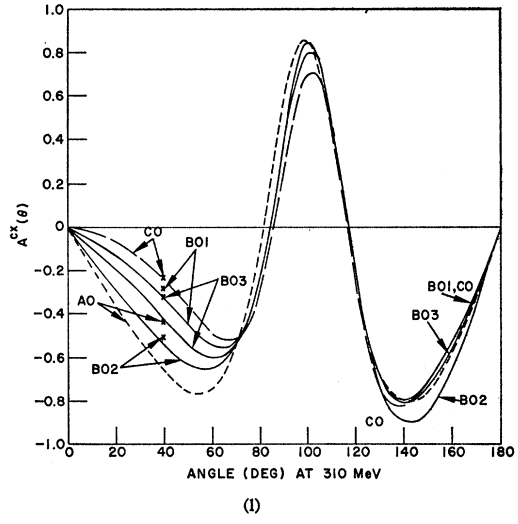

(l)

search. (d) The points are 310-MeV data from J. H. Foote, O. Chamberlain, E. H. Rogers, H. M. Steiner, C. E. Wiegand, and I. Ypsilantis, Phys. Rev. **122**, 948 (1961). The crosses at 40° indicate how the solutions changed when new data were included and the real parts of the forward amplitudes were used as data. (e) The points are 310-MeV data from the same source as (b) above. (f) The one point is a 310-MeV datum from R. E. Hill, N. E. Booth, R. J. Esterling, D. L. Jenkins, N. H. Lipman, H. R. Rugge, and O. T. Vik, Bull. Am. Phys. Soc. **9**, 410 (1964) [superseded by R. E. Hill (private communications)]. The crosses at 30 and 140° indicate how the solutions changed when new data were included and the real parts of the forward amplitudes were used as data. (g)–(l) The crosses indicate how the solutions changed when new data were included and the real parts of the forward amplitudes were used as data.

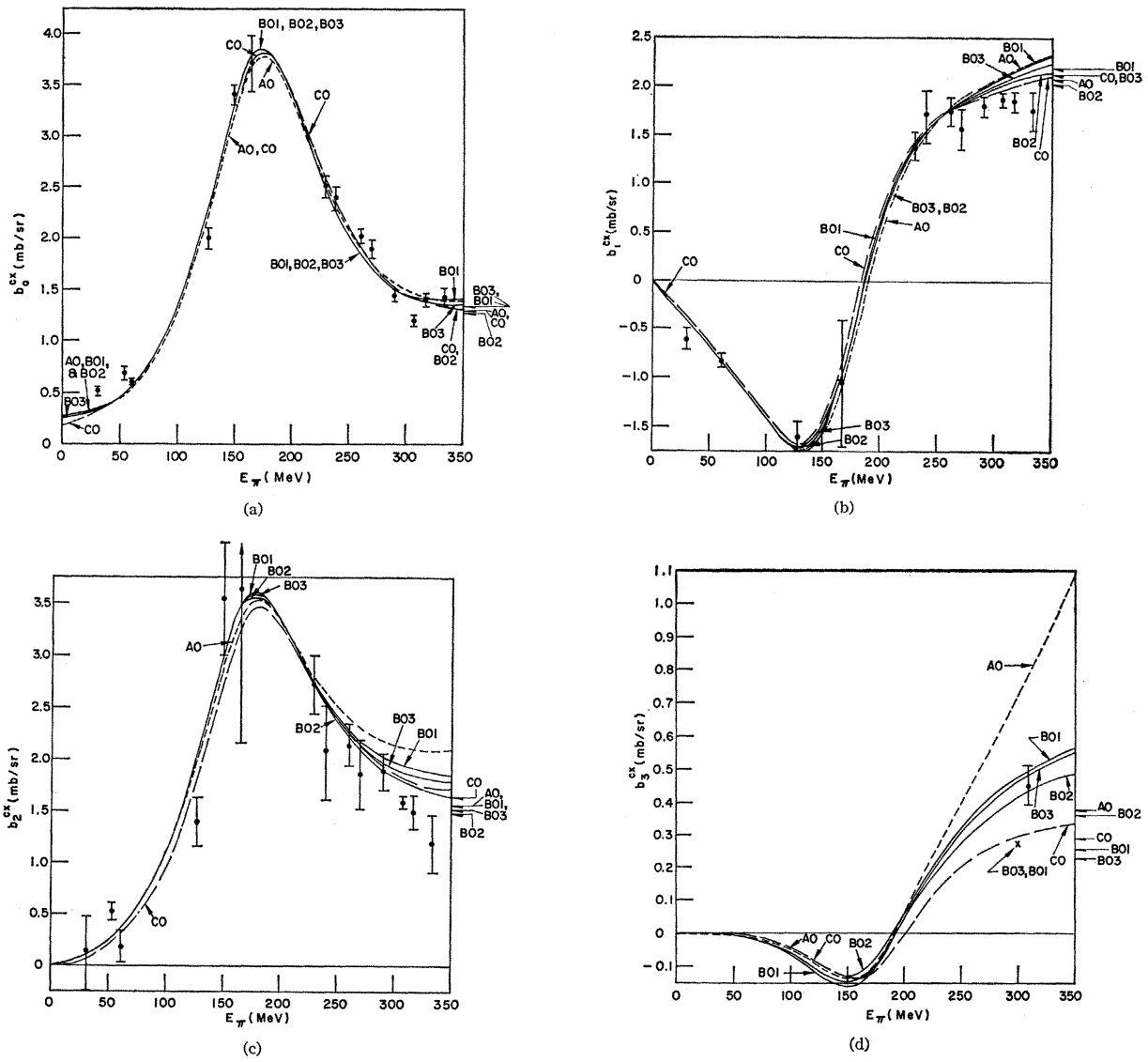

FIG. 7. (a)–(c) The solutions' predictions of the charge-exchange Legendre polynomial coefficients. The points are from many sources (see Ref. 1). Renormalization of the data in the searches is not shown. (d) The point at 313 MeV is from R. J. Kurz and D. L. Lind, Lawrence Radiation Laboratory (Berkeley) UCRL-11548, 1964 (unpublished). The arrows at the right edge and the cross at 300 MeV indicate how the solutions changed when new data were included and the real parts of the forward amplitudes were used as data.

nomial coefficients for the solutions, where

$$\sigma^{cx}(\theta)=\sum_{n=0}^{2l_m} b_n P_n(\cos\theta).$$

The experimental data points, except the 310-MeV points, plotted in Fig. 7 were obtained by the experimentalists using the assumption that only S and P waves contribute to the charge-exchange scattering. (We would much prefer having charge-exchange data in terms of values at different angles rather than Legendre polynomial or $\cos\theta$ series coefficients.) Figure 1 indicates that this assumption is not valid higher than $\sim$150 MeV. However, these data were used in the search and were calculated using only the S and P waves in the computation of χ^2. The curves in Fig. 7 were calculated using all partial waves through F waves. Therefore, we do not expect good agreement at the higher energies in Fig. 7. The agreement was better in the computation of χ^2. The fourth coefficient at 310 MeV as determined by Kurz and Lind[7] favors the B solution and disfavors the A solution. The experimental values of the second and third coefficients near the end of the energy range disfavor the A solution, also.

[7] R. J. Kurz and D. L. Lind, Lawrence Radiation Laboratory (Berkeley) UCRL-11548, 1964 (unpublished).

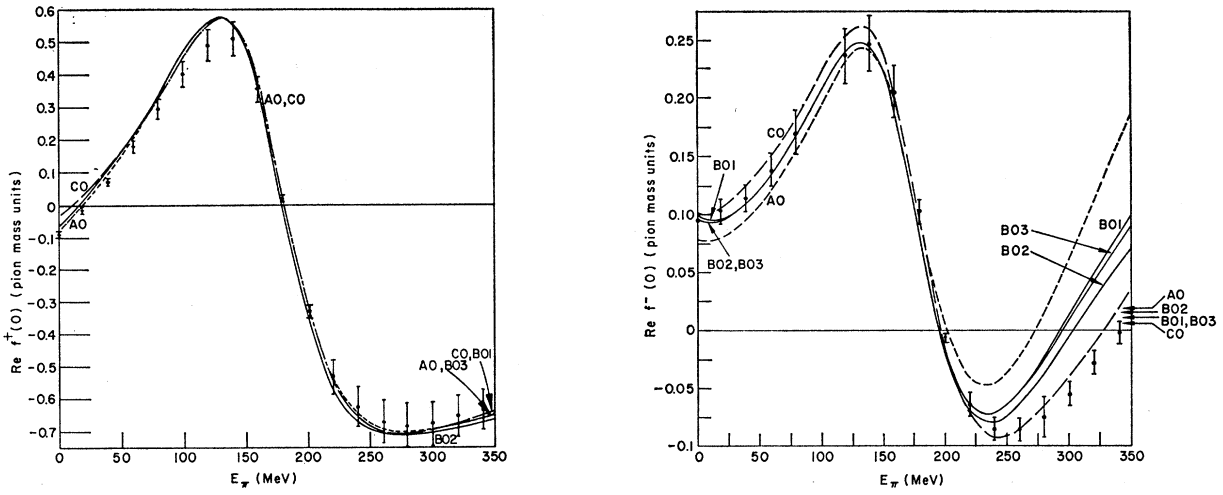

FIG. 8. The solutions' predictions of the real parts of the forward amplitudes. (a) The points at 20-MeV intervals are from G. Höhler, G. Ebel, and J. Giesecke, Z. Physik **180**, 430 (1964). These values were not used as data in the search. (b) The points at 20-MeV intervals are from the same source as (a). These values were not used as data in the search. The arrows at the right indicate how the solutions changed when new data were added and these values were used as data.

IV. FORWARD SCATTERING AND NEW DATA

Figure 8 gives the prediction of the real parts of the forward $\pi^{\pm}-p$ amplitudes as predicted by the solutions versus the dispersion relation calculation of Höhler *et al.*,[8] where

$$\mathrm{Re}f(0)=\frac{1}{k}\sum_{l=0}^{\infty}[(l+1)\,\mathrm{Re}A_{l+}+l\,\mathrm{Re}A_{l-}].$$

It is seen that these "data" favor the C solution and disfavor the A solution. The forward cross sections as computed from the forward dispersion relation calculation of Niederer[9] were used as data in our analysis. The Höhler and Niederer forward cross sections are in agreement with each other. However, since we used the forward cross sections rather than the real parts of the forward amplitudes, we may not be fitting the real parts of the forward amplitudes very well. That is, since

$$\sigma(0)=[\mathrm{Re}f(0)]^2+[(k/4\pi)\sigma_T]^2,$$

in the regions where the second bracket is much larger than the first we are essentially fitting total cross sections rather than the real parts of the forward amplitudes. Thus, it is understood why the solutions

TABLE II. Values of the phase shifts at 345 MeV when $\mathrm{Re}f^{\pm}(0)$ and new data are used. The last four lines contain solution χ^2's.

Phase	*AO*	*BO1*	*BO2*	*BO3*	*CO*
S_{11}	13.30	12.61	14.83	13.56	10.68
S_{31}	−24.75	−25.04	−25.24	−24.74	−24.06
P_{11}	31.40	31.22	30.64	31.30	29.44
P_{31}	−11.63	−14.02	−12.71	−13.49	−15.26
P_{13}	−3.38	−4.50	−4.27	−4.31	−5.34
P_{33}	141.17	141.62	141.62	141.62	141.21
D_{13}	6.87	7.84	6.89	7.56	8.29
D_{33}	−2.12	−3.79	−1.83	−3.35	−4.48
D_{15}	1.38	0.406	0.883	0.472	0.608
D_{35}	−0.138	1.90	0.774	1.38	1.83
F_{15}	1.85	2.40	1.06	2.13	2.68
F_{35}	−1.06	−2.14	−0.188	−1.82	−2.31
F_{17}	−1.41	−1.66	−0.189	−1.69	−1.37
F_{37}	2.49	3.57	0.72	3.24	4.39
χ^2	1228	1174	1243	1169	1126
χ^2 (expected)	462	453	461	453	447
χ^2/χ^2 (exp.)	2.66	2.59	2.70	2.58	2.52
χ^2 (renormalization)	179	106	106	106	135

TABLE III. Proposed experiments at 310 MeV to distinguish among solutions A, B, and C.

Observable	Approximate angle (deg)	Approximate accuracies: Original solutions (mb/sr for $\sigma(\theta)$)	Approximate accuracies: Altered solutions (mb/sr for $\sigma(\theta)$)
$\sigma^+(\theta)$	180	±0.05	±0.05
$\sigma^-(\theta)$	20	±0.05	±0.01
$\sigma^-(\theta)$	180	±0.03	±0.005
$\sigma^{cx}(\theta)$	0	±0.5	±0.05
$P^+(\theta)$	40	±0.05	±0.03
$P^-(\theta)$	50	±0.03	±0.03
$P^{cx}(\theta)$	140	±0.05	±0.05
$R^+(\theta)$	50	±0.06	±0.04
$R^-(\theta)$	70	±0.05	±0.03
$R^{cx}(\theta)$	80	±0.05	±0.03
$A^+(\theta)$	40	±0.03	±0.03
$A^-(\theta)$	40	±0.06	±0.02
$A^{cx}(\theta)$	40	±0.06	±0.04

[8] G. Höhler, G. Ebel, and J. Giesecke, Z. Physik **180**, 430 (1964).

[9] J. Niederer (private communication).

TABLE IV. Rating of the solutions (lowest score is favored).

Solution	Original solutions: χ^2 / χ^2 exp.	χ^2 renormalization	Agreement with best 300–700-MeV solution	Agreement with $\mathrm{Re}f^-(\theta)$	Total	Altered solutions: χ^2 / χ^2 exp.	χ^2 renormalization	Agreement with best 300–700-MeV solution	Total	Grand total
AO	5	5	2	5	17	4	5	1	10	27
BO1	1	1	3	4	9	3	1	4	8	17
BO2	4	2	1	2	9	5	1	2	8	17
BO3	1	3	3	3	10	2	1	3	6	16
CO	3	4	5	1	13	1	4	5	10	23

give widely varying results for $\mathrm{Re}f(0)$ near the end of the energy range (k increasing).

Recently Kurz and Lind[7] have reported σ^{cx} at 313 MeV and Troka[10] has reported $\sigma^+(\theta)$ at 247.5 MeV. The former data are plotted in Fig. 6 and the latter are plotted in Fig. 5.

We included these new data and the Höhler[8] real parts of the forward amplitudes in a data selection of 490 data and did the analysis again. Errors of 10% were attached to the Höhler "data." These are probably too-small errors, but we wanted to see if the solutions would coincide when fitting the real parts of the forward amplitudes is forced. Table II shows the values obtained for the phase shifts at 345 MeV. The values at 345 MeV are also shown by arrows at the right-hand edges of Fig. 1. It is seen that the solutions are brought closer together. Arrows at the right-hand edge of the second part of Fig. 8 show how well the altered solutions fit the 340-MeV $\pi^- - p$ forward amplitude "data." Arrows and crosses in Fig. 6 indicate how the inclusion of the new data and of $\mathrm{Re}f^{\pm}(0)$ as data altered the predictions of the observables.

V. PROPOSED EXPERIMENTS

The solutions differ most near the end of the energy range. We shall consider experiments at about 310 MeV, since many data are already available at that energy. Figure 6 suggests the very difficult, if not impossible, experiments listed in Table III. The 310-MeV $P^-(\theta)$ data (Fig. 6) at the lowest measured angles ($\sim 115°$) are inconsistent with the solutions reported here. It appears that these data should be remeasured.[11] The $P^{cx}(\theta)$ datum at 30° is slightly lower than most of our solutions predict. The two $\sigma^-(\theta)$ data for $\theta > 160°$ appear to be in error; new data in this angular region would be helpful. The 313-MeV $\sigma^{cx}(\theta)$ data are low at high angles, with respect to our solutions. Inclusion of these 313-MeV data in the data selection did not effect a better fit to them. Kurz and Lind[7] noted in reporting these data that they are barely compatible with the $\pi^{\pm} - p$ data. An independent measurement of $\sigma^{cx}(\theta)$ at 310 MeV would be desirable. To our knowledge no values of the spin-rotation parameters, $A(\theta)$ and $R(\theta)$, have ever been measured at any energy. A polarized target is required for their measurement.[6] The accuracies listed in Table III would probably be impossible to obtain for many years.

VI. CONCLUSIONS

Table IV is an attempt to assign a crude quantitative rating to the solutions *AO*, *BO1*, *BO2*, *BO3*, and *CO* based on their relative χ^2's, the relative contribution to χ^2 due to the differential cross section normalization parameters,[1] agreement with the best 300–700-MeV solution (unpublished), and agreement with the Höhler calculation[8] of $\mathrm{Re}f^-(0)$. The solutions *BO1*, *BO2*, *BO3* are preferred over *AO* and *CO* on the basis of this rating. The observables listed in Table III that could best be used to distinguish among *BO1*, *BO2*, and *BO3* are $P^+(40°)$, $P^{cx}(140°)$, $R^+(50°)$, $R^{cx}(80°)$, $A^+(40°)$, and $A^{cx}(40°)$; which indicates that the differences among the solutions in the $T=\frac{3}{2}$ states are more important than their differences in the $T=\frac{1}{2}$ states. We would recommend *BO3* as the best available solution.

ACKNOWLEDGMENTS

The authors wish to thank Dr. M. J. Moravcsik for his continuous support of these analyses. Discussions with Dr. V. Perez-Mendez have been useful. Eldon Halda has contributed much in the way of computer programming, for which we are grateful. Dr. Sidney Fernbach of the Theoretical and Computational Divisions at Lawrence Radiation Laboratory, Livermore, has provided the large amounts of computer time necessary for these calculations.

[10] W. K. Troka, Lawrence Radiation Laboratory (Berkeley) UCRL-11537, 1964 (unpublished).

[11] P. Auvil and C. Lovelace, Nuovo Cimento 33, 473 (1964).